

# Hidden Defect Pairs: Objects Invisible in Low-Energy Electron Scattering

A. A. Gorbatsevich\*

*Moscow State Institute of Electronic Technology (Technical University)  
Zelenograd, Moscow, 124498, Russia*

(Dated: October 26, 2018)

Objects composed of lattice defects exist within a one-dimensional tight-binding model whose electron reflection coefficient in the low-energy case is equal to zero. Localized states are absent as well. The effective mass concept explains this not as some kind of reflectionless potential but as homogeneous medium, in which effective object size collapses. Without making effective mass approximations a new type of resonance is observed, in which the reflection coefficient becomes zero at a certain energy.

PACS numbers: 03.65.Nk, 71.55.Cn, 71.55.Eq, 72.10.Fk

Electron scattering is a useful tool for studying atomic as well as condensed matter objects. The internal structure of these objects can manifest itself through various kinds of resonances. The long-wave-length case of the effective mass model (EMM) allows treating condensed matter as continuous medium. In this case all known resonances of elastic electron scattering have direct optical (or microwave) analogues originating from the interference of waves scattered in extended reflecting systems: resonant tunneling and Fabri-Perro resonances, virtual-state resonances in over-barrier electron transmission in semiconductor heterostructures (Ramsauer-Townsend-like resonances) and resonances in light transmission through thin refracting plates, Fano resonances both in electron and microwave multimode waveguides.

In this letter we demonstrate the existence of a new type of electron transmission resonance. We show that extended microscopic objects can exist in a one-dimensional lattice model which possess anomalous transparency in the case of electron scattering - they are invisible in the low-energy case. These objects are pairs of defects (hidden defect pairs - HDP) with antisymmetric defect potentials located at unequivalent sites at certain distances and in a special pattern. The transparency coefficient of an HDP equals unity without any phase factors and bound states are absent. This fact sets the described objects apart from the well-known reflectionless potentials. In the continuous case described by EMM the effective size of an object can essentially differ from its real microscopic size. Anomalous transparency of an HDP corresponds to the collapse of effective defect pair size in the continuous case. The continuous representation of a separate defect is known to be a delta-function potential. However an HDP in this case may appear as a structureless homogeneous medium - as if the two defects cancel each other. Without the use of effective mass approximation microscopic objects also can be characterised by an effective size which in this case becomes energy dependent. At a certain energy this size becomes zero and a resonance of a new type takes place manifesting itself through the absence of electron reflection.

Consider a one-dimensional tight-binding model with both bond and on-site alternation. Different atoms in the unit cell are denoted by index  $j$  ( $j = 1, 2$ ). Let two defects (impurities) be located at sites  $M_1$  and  $M_2$ , occupied in a host lattice by atoms 1 and 2. The Hamiltonian of the model is:

$$\hat{H} = \sum_{j=1,2} \sum_{n_1, n_2} [\varepsilon_j C_{j n_j}^\dagger C_{j n_j} - C_{1 n_1}^\dagger (t_+ C_{2 n_1+1} + t_- C_{2 n_1-1}) + \varepsilon_j^* C_{M_j}^\dagger C_{M_j} + h.c.]. \quad (1)$$

Here  $C_{j n_j}^\dagger$  ( $C_{j n_j}$ ) is the electron creation (annihilation) operator at site  $n_j$ ,  $n_1 = 2m$ ,  $n_2 = 2m + 1$  ( $m$  - integer),  $\varepsilon_{1,2}$  are on-site energies of bulk material, while  $\varepsilon_{1,2}^*$  are on-site defect energies and  $t_\pm = t_1 \pm t_2$  are alternating hopping integrals. Hopping integrals for defect atoms are taken to be the same as in the bulk. The model (1) describes  $\Delta_{3(4)}$  hole states originating from atomic p-orbitals at the Brillouin zone (BZ) center in semiconductors with zinc-blend structure [1, 2] as well as Peierls insulators with both bond and site alternation (asymmetric Peierls model). A simplified version of this model with  $\varepsilon_1 = \varepsilon_2$  (symmetric Peierls model) was successfully used to describe electronic states in polyacetylene (PA) [3]. The energy spectrum of the model (1) without defects possesses two (lower (L) and upper (U)) branches:

$$E_{U,L}(k) = \varepsilon_0 \pm \sqrt{\delta^2 + 4t_1^2 \cos^2(ka) + 4t_2^2 \sin^2(ka)} = \varepsilon_0 \pm E(k). \quad \text{Here } \varepsilon_0 = \frac{1}{2}(\varepsilon_1 + \varepsilon_2), \quad \delta_0 = \frac{1}{2}(\varepsilon_1 - \varepsilon_2) \text{ and } a \text{ - is the interatomic distance, which we take to be equal for adjacent bonds. For } t_2 > t_1 \text{ the energy band extrema are at the BZ center. The wave functions for the upper band are } c_{1,2k} U = u_k, -v_k e^{-i\varphi_{1,2}(k)}, \text{ where the phase factors } \varphi_{1,2}(k) \text{ are related to each other by the expression}$$

$$\varphi_2(k) - \varphi_1(k) = \vartheta(k), \quad \vartheta(k) = \arctan(\theta \tan(ka)), \quad (2)$$

with  $\theta = t_2/t_1$ . Coefficients  $u$  and  $v$  have the standard form of canonical transformation coefficients:  $u_k, v_k = [(1/2)(1 \pm \delta/E(k))]^{\frac{1}{2}}$  [4]. For the lower band the solution is obtained by reversal:  $u \rightarrow -v, v \rightarrow u$ .

Consider a scattering solution of the Hamiltonian (1), in the form:  $c_{1,2n} = c_{1,2k} e^{ikna} + r c_{1,2-k} e^{-ikna}$ ,  $n <$

$M_1$ ;  $c_{1,2m} = tc_{1,2k}e^{ikma}$ ,  $m > M_2$ . After some algebraic manipulations we obtain the following expressions

$$r = -e^{2ikM_1 - 2i\zeta_a} \frac{(\Delta_1 \Delta_2 u_k v_k + i\Delta_k - U_k) \sin[L_{eff}(k)k] - \Delta_k + U_k \cos[L_{eff}(k)k]}{\Delta_1 \Delta_2 u_k v_k \sin[L_{eff}(k)k] - (\Delta_k + + 2iu_k v_k U_k) U_k e^{-iL_{eff}(k)k}}, \quad (3)$$

$$t = -e^{-iL_{eff}(k)k} \frac{2iu_k v_k U_k^2}{\Delta_1 \Delta_2 u_k v_k \sin[L_{eff}(k)k] - (\Delta_k + + 2iu_k v_k U_k) U_k e^{-iL_{eff}(k)k}}, \quad (4)$$

where

$$\Delta_{1,2} = \varepsilon_{1,2}^* - \varepsilon_{1,2}, \quad \Delta_{k\pm} = \Delta_1 v_k^2 \pm \Delta_2 u_k^2, \\ U_k = t_2 \sin[\vartheta(k)] \cos(ka) - t_1 \cos[\vartheta(k)] \sin(ka).$$

$\Delta_j > 0$  ( $< 0$ ) corresponds to donor- (acceptor-) like impurity. In (3) the effective size of the defect pair is introduced.

$$L_{eff}(k) = L_0 - \frac{1}{k} \vartheta(k), \quad (5)$$

where  $L_0 = (M_2 - M_1)a$ . Under the condition

$$\Delta_1 v_k^2 = -\Delta_2 u_k^2 \quad (6)$$

$\Delta_{k+}$  and the last term in the numerator of (3) both become zero and the reflection coefficient becomes proportional to  $\sin[L_{eff}(k)k]$ . At  $L_{eff}(k) = 0$  resonance takes place:  $r = 0$  and  $t = 1$ . In the symmetric Peierls model ( $\delta = 0$ ) the condition (6) is energy independent and becomes  $\Delta_1 = -\Delta_2$ . In the asymmetric Peierls model the  $u_k$  and  $v_k$  factors in (6) depend upon energy and the resonance is observed only if the conditions (8) and  $L_{eff} = 0$  are satisfied at one and the same energy.

In the case

$$ka \ll 1, \quad \vartheta(k) \approx \theta ka \ll 1, \quad (7)$$

which corresponds to the values of  $k$  within EMM  $L_{eff}(k) = L_{eff} = L_0 - a\theta$  then the function  $\sin[L_{eff}(k)k]$  in (3) becomes  $\sin[(L_0 - a\theta)k]$ . Hence at large enough value of  $\theta$  (or at small enough value of  $L_0$ ) such that  $L_{eff} = 0$  the reflection coefficient  $r$  identically equals zero at all values of  $k$  within the framework of EMM.

For  $t_1 > t_2$  (as is the case for PA) the energy band extrema are at the BZ boundary. The continuous (EMM) case for such a model corresponds to small wave vectors measured from the extremum points at  $k = \pm\pi/a$ . It can be shown that for such wave-vectors formulas (3), (4) are maintained with the following modifications: hopping integrals  $t_1$  and  $t_2$  are interchanged (parameter  $\theta = t_1/t_2$ ) and the reflection coefficient acquires insignificant phase factor.

for the reflection ( $r$ ) and transmission ( $t$ ) coefficients in the upper band:

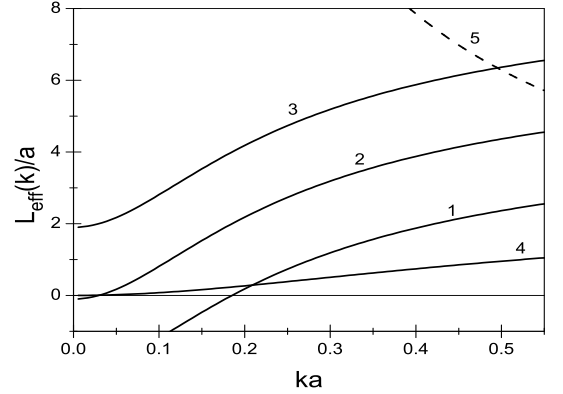


FIG. 1: Dependence of effective interdefect distance  $L_{eff}(k)$  on wave-vector. Curve 1 –  $\theta = 7.1, L_0 = 5$ ; 2 –  $\theta = 7.1, L_0 = 7$ ; 3 –  $\theta = 7.1, L_0 = 9$ ; 4 –  $\theta = 3, L_0 = 3$ . Curve 5 –  $kL_{eff}(k) = \pi$ .

The dependence of the effective length  $L_{eff}(k)$  on the wave-vector is shown in Fig. 1. The parameter  $\theta$  is usually accepted to be 7.1 in band-structure calculations for PA [3]. In group IV elements and A3B5 compounds this parameter varies from 2 to 3 [1, 5].

To understand the physical nature of the described phenomenon consider continuous case where a point defect can be reproduced by a  $\delta$ -function potential. For two  $\delta$ -functions located at points  $x_1$  and  $x_2$  it can be shown that in continuous EMM the reflection coefficient  $r$  exactly matches the result (3) in the case (7) with  $L_{eff}(k)$  being replaced by  $x_2 - x_1$ . For equal in magnitude and reverse in sign  $\delta$ -potentials  $r$  exhibits usual virtual state resonance at  $k(x_2 - x_1) = \pi$  but it becomes identically zero if and only if  $x_1 = x_2$ . Hence the analogous behavior of the reflection coefficient in the discrete model (1) can be interpreted as if the effective size of defect pair in the continuous case is determined not by real physical defect separation  $L_0$ , but rather by the effective length  $L_{eff}(k)$  (5), which can undergo collapse at certain values of the parameters.

One-dimensional objects with  $r \equiv 0$  (reflectionless potentials) are known in physics [6, 7]. However the transmission coefficient of a reflectionless potential possesses a nonzero phase-factor:  $t = e^{i\phi}$ . The phase  $\phi$  is determined by the location of scattering amplitude poles in the complex wave-vector plane which are related to energies of bound states. The phase of the transmission coefficient as well as the bound states can be used to detect the existence of reflectionless potential. The potentials with zero effective size described in the present paper are much more hidden objects. The transmission coefficient  $t$  (4) at the condition  $L_{eff}(k) = 0$  (at  $\Delta_+ = 0$ ) equals unity without any phase factor. Bound states don't exist either: it can be shown that dispersion relation for bound state energy  $r^{-1}(k = i\kappa) = 0$  has no nontrivial solutions at  $L_{eff}(k) = 0$ . Hence HDP are completely invisible in the long-wave-length case. In this case they appear as structureless homogeneous medium and in this sense they have no optical analogue. On the other hand analogous objects can be constructed in photonic crystals with dielectric permittivity periodically varying in space. Taking into account deviations from continuous case (non-parabolicities) HDP manifest themselves as broad resonances at anomalously low energies.

Consider two defects located at equivalent lattice sites  $M_1$  and  $M_2$  (e.g. both occupied in a host lattice by atoms of sort 1) with energies  $\epsilon_1^* = \epsilon_1 + \Delta_1$  and  $\epsilon_2^* = \epsilon_1 + \tilde{\Delta}_1$  respectively. It can be shown that the reflection coefficient  $\tilde{r}$  in this case can be obtained from the expression (3) with the following substitutions:

$$\tilde{r}(k) = r(k, \Delta_2 u_k \rightarrow \tilde{\Delta}_1 v_k, U_k v_k \rightarrow U_k u_k, L_{eff}(k) \rightarrow L_0). \quad (8)$$

The main difference between (8) and (3) is that in (8) the effective length  $L_{eff}(k)$  is replaced by the physical microscopic length  $L_0 = (M_2 - M_1)a$ . Hence any anomalies related to the possible collapse of a defect pair in the continuous case are absent.

The square modulus of the reflection coefficient  $|r|^2$  in the symmetric Peirls model with antisymmetric defect potential as a function of wave-vector is shown in Fig.2. The parameters of curve 4 satisfy the condition  $L_0 = \theta$  of exact defect pair collapse in macroscopic case  $ka \ll 1$ . In this case  $r(k=0) = 0$ . All the other curves become unity at  $k \rightarrow 0$ . From Fig.2 one can see that even in the model where  $L_{eff}(k)$  doesn't become zero (curve 3) the decrease of the effective defect pair size results in the formation of a pronounced minimum in the  $r(k)$  curve at small energies. The parameters for curve 5 are the same as for curve 2 except for location of right atom which is shifted half a lattice period to the right. The resonance observed in curve 3 at  $ka = 0.495$  is a virtual state resonance corresponding to the intersection of curves 3 and 5 in Fig.1. The resonance in curve 5 is also a virtual state resonance at  $k = \pi/L_0$  ( $L_0 = 8a$ ).

The results obtained above mean that the location of

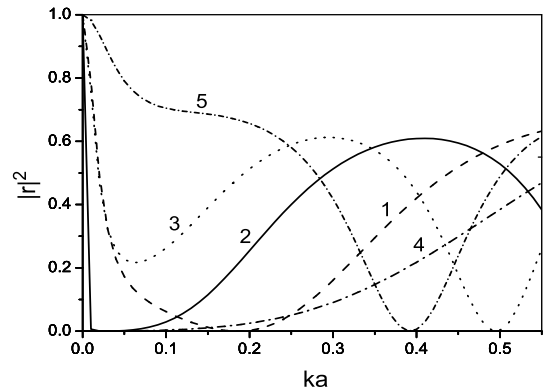


FIG. 2: Dependence of reflection coefficient on wave-vector in SPM with  $\delta = 0$ ,  $t_1 = 3.2eV$  ( $t_1 > t_2$ ). For curves 1-4 other parameters and labeling are the same as in Fig.1. Curve 5 corresponds to pair of defects at equivalent lattice sites (8),  $\theta = 7.1$ ,  $L_0 = 8a$ .

the defect in continuous model can essentially differ from its physical microscopic position. The description of a point defect in the continuous regime is a particular case of an interface description. An interface can be characterized in continuous EMM by means of a transfer matrix  $\hat{T}$  which connects wave functions and their derivatives on both sides of the interface located at  $x_0$  [8, 9]:

$$\begin{pmatrix} \varphi \\ \nabla \varphi \end{pmatrix}_+ = \hat{T} \begin{pmatrix} \varphi \\ \nabla \varphi \end{pmatrix}_- = \begin{pmatrix} T_{11} & T_{12} \\ T_{21} & T_{22} \end{pmatrix} \begin{pmatrix} \varphi \\ \nabla \varphi \end{pmatrix}_- \quad (9)$$

The parameters of the transfer matrix  $\hat{T}$  can be calculated using an extrapolation of the site amplitudes at the interface location [8, 10]. More rigorously the off-diagonal elements of  $\hat{T}$  can be calculated in a pseudopotential model [11]. However to get information about the precise location of the interface you should use another approach. Let's express the scattering data ( $r$  and  $t$ ) as a power series in wave-vector for both an EMM with boundary condition (9) and a microscopic model. Within the EMM take only terms up to the first order of magnitude. Equate the coefficients at the terms of the same order in micro- and macroscopic case and obtain the transfer matrix parameters from the scattering data for microscopic model. You can also deduce in this way the interface location  $x_0$  which enters the equations for scattering data in linear combination with the wave-vector. In particular  $T_{21}$  can be obtained from the expression for the transmission coefficient at zero wave-vector of the incident wave:  $T_{21} = -2ikt^{-1}_{k \rightarrow 0}$ . It can be shown that for a heterointerface of two different materials and nonzero (and not small)  $T_{21}$  in (9) the number of unknown parameters is greater than the number of equations resulting from the extraction procedure. Hence the interface location  $x_0$  can't be determined. The situation is differ-

ent for a solitary defect. In this case  $T_{11} = T_{22} = 1$  and the number of unknown parameters is reduced. Let the defect in microscopic model be located at site  $M_1$ , which we choose as a coordinate origin:  $x_0 = M_1 a + \Delta x_0$ . Decomposition of the reflection coefficient in EMM (9) for the plane wave  $e^{ik(x-\delta)}$  ( $\delta$  - phase factor) incident from the left in terms of the transfer matrix parameters then takes the form:

$$r \approx -e^{ikM_1 a} [1 + 2ik(\frac{1}{T_{21}} + \Delta x_0 - \delta) + \dots]. \quad (10)$$

The reflection coefficient  $r$  in the microscopic model 1 for the defect replacing atom 1 of host material is:

$$r = -e^{2i(kMa - \varsigma_1)} \Delta_1 v_k / (\Delta_1 v_k - 2iu_k U_k), \quad (11)$$

where the parameters  $\Delta_1$ ,  $u_k$  and  $U_k$  are the same as in (3). From the expression for the transmission coefficient one gets  $T_{21} = (v_0 \Delta_1 t_1) / (u_0 (t_2^2 - t_1^2) a)$  (here we assume  $t_2 > t_1$ ). Comparison of (10) with the decomposition of (11) in powers of  $ka$  provides for the location of the defect:  $x_{01}^{(1)} - \delta = M_1 a - \varsigma_1$ . The same procedure repeated for the defect replacing the type 2 atom located at site  $M_2$  gives:  $x_{02}^{(2)} - \delta = M_2 a - \varsigma_2$ . Subtracting  $x_{02}^{(2)}$  from  $x_{01}^{(1)}$  eliminates the unspecified parameter  $\delta$  and obtains for the effective length  $L_{eff} = x_{02}^{(2)} - x_{01}^{(1)} = (M_2 - M_1 - \theta) a$  - the same expression as (5) in the case (7). If both atoms are in equivalent positions then their effective separation in the continuous case exactly coincides with their real physical separation in the microscopic model  $x_{02}^{(1)} - x_{01}^{(1)} = (M_2 - M_1) a$ . This fact explains the radical difference between the reflection coefficients of defect pairs (3) and (8) when their sizes differ only by half a lattice period. The unknown constant - phase factor  $\delta$  can be determined by applying an extraction procedure to the heterointerface. In this case additional information can be obtained from the decomposition of  $r'$  in powers of wave-vector ( $r'$  is the reflection coefficient for the wave incident from the right). As a result you obtain  $\delta = (\varsigma_1 + \varsigma_2)/2$  and  $x_0^{(1,2)} = Ma \pm \theta/2$ . Therefore defects located at equivalent (nonequivalent) sites shift in macroscopic picture in the same (opposite) direction(s).  $\Delta_3$  and  $\Delta_4$  states in group IV and A3B5 semiconductors differ by the sign of  $\theta$ . Hence the collapse of a defect pair for the  $\Delta_3$  states will be accompanied by a doubling of the effective defect pair size for the  $\Delta_4$  states and vice versa.

The physical nature of the described effect lies in the space-inversion asymmetry of the model (1). This microscopic asymmetry causes asymmetric wave function distortions (with respect to the distribution of wave-function in the virtual reference symmetric model). Within the framework of continuous EMM approach condensed matter objects are structureless entities and their description is the same for both symmetric and asymmetric microscopic models. Hence the only way to describe

these microscopic asymmetric distortions in the continuous case is to shift the location of the defect in respect to its position in the reference symmetric case.

To conclude, the extended microscopic object invisible in low-energy electron scattering - HDP - was constructed. Favorable conditions for the formation and observation of an HDP can be provided by electrical annealing: prolonged current transmission. The association of separate defects into an HDP results in a local decrease of resistivity. In regions with smaller HDP concentration and higher resistivity Joule heat would enhance diffusion which helps HDP formation with subsequent reduction of resistivity and diffusion in this region. Finally the whole specimen can transform into HDP enriched phase. These pairs can be distributed chaotically and form a disordered conductor without localization (a hidden defect structure). Anomalous macroscopic behavior of scattering data results from the underlying spatial asymmetry. This scenario seems to be quite universal and proposes a variety of "invisible" objects to exist in condensed matter. Another objects of this type are a quantum well in the model (1) with foreign atoms at the heterojunctions and a defect pair in the generalized Kronig-Penney model without center of inversion, which will be described in a separate paper.

The author acknowledges the support of Russian Foundation for Basic Research and Russian Ministry of Science and Education and helpful discussions with I.V.Tokatly.

---

\* Electronic address: aag@qdn.miee.ru

- [1] P. Y. Yu and M. Cardona, *Fundamentals of Semiconductors: Physics and Materials Properties* (Springer-Verlag, Berlin, 2001).
- [2] In semiconductor notations [1]:  $t_1 \rightarrow V_{xx}$  and  $t_2 \rightarrow V_{xy}$  and indices 1 and 2 denote anion and cation atoms.
- [3] A.J. Heeger, S. Kivelson, J.R. Schrieffer and W.-P. Su, *Rev. Mod. Phys.* **60**, 781 (1988).
- [4] Amplitudes  $c_k, k+\pi/a$  usually used in Peierls model for PA description are:  $c_k, k+\pi/a = \frac{1}{\sqrt{2}}(c_1 k \pm c_2 k)$ .
- [5] P. Vogel, H.P. Hjalmarson and J.D. Dow, *J.Phys. Chem. Solids* **44**, 365 (1983).
- [6] L.D. Landau and E.M. Lifshitz, *Quantum Mechanics* (Pergamon Press, Oxford, 1977).
- [7] C. Mora, R. Eger and A.O. Gogolin, *Phys. Rev. A* **71**, 052705 (2005).
- [8] T. Ando and S. Mori, *Surf. Sci.* **113**, 124 (1982); T. Ando, S. Wakahara and H.Akera, *Phys. Rev. B* **40**, 11609 (1989).
- [9] I.V. Tokatly, A.G. Tsibizov and A.A. Gorbatshevich, *Phys. Rev. B* **65**, 165328 (2002).
- [10] E.L. Ivchenko, A.Yu. Kaminski and U. Rossler, *Phys. Rev. B* **54**, 5852 (1996); E.L. Ivchenko, A.A. Toropov and P.Voisin, *Fiz. Tverd. Tela (St.Petersburg)* **40**, 1925 (1998) [*Phys. Solid. State* **40**, 1748 (1998)].
- [11] B.A. Foreman, *Phys. Rev. Lett.* **81**, 425 (1998).